Date of publication xxxx 00, 0000, date of current version xxxx 00, 0000.

Digital Object Identifier xxxx

Design of Reconfigurable SDR Platform for Antenna Selection Aided MIMO Communication System

PEICHANG ZHANG[1], JIAJUN XU[1], SHIDA ZHONG[1], HAOGANG FENG[1], LEI HUANG[1], TAO YUAN[1], and JIANKANG ZHANG[2](Senior Member, IEEE)

[1]College of Electronics and Information Engineering, Shenzhen University, Shenzhen 518060, China. (e-mail: pzhang@szu.edu.cn; xujiajun2017@email.szu.edu.cn; shida.zhong@szu.edu.cn; fenghaogang@email.szu.edu.cn; lhuang@szu.edu.cn; yuantao@szu.edu.cn)
[2]School of Electronics and Computer Science, University of Southampton, Southampton SO17 1BJ, U.K. (e-mail: jz09v@ecs.soton.ac.uk)

Corresponding author: Shida Zhong (e-mail: shida.zhong@szu.edu.cn).

This work is supported in part by the Natural Science Foundation of China under Grants 61601304, U1713217, U1501253, 61801297, 61801302 and 61571401, in part by the Foundation of Shenzhen under Grant JCYJ20170302142545828, and in part by the Foundation of Shenzhen University under Grant 2016057 and 2019120.

ABSTRACT In recent years, antenna selection (AS) has become one of the most popular research topics for massive multiple-input multiple-output (MIMO) system due to its capability of reducing the number of radio frequency chains utilized for MIMO communications, while remaining the MIMO advantages, such as increased bandwidth efficiency and reliability. In this paper, an efficient norm-based AS (NBAS) algorithm is investigated and implemented in the software defined radio (SDR) MIMO communication platform, which consists of field-programmable gate arrays (FPGAs). Owing to the high freedom and fast reconfigurable FPGA hardware, the SDR MIMO communication platform is capable of developing prototype of NBAS-aided MIMO system. More specifically, the implemented NBAS aided SDR MIMO system is capable of achieving uplink communication from users to the base station via time division duplex (TDD). A time-varying fading channel generation model is designed for SDR MIMO platform to enrich our experimental results. Additionally, a novel multiplexer (MUX) circuit module is designed and implemented to enhance the hardware performance of the FPGA in term of delay and resource usage. The results show that by implementing the low-complexity NBAS, the channel capacity performance of the SDR MIMO system can be significantly improved by around 15%. It is also showed that our proposed optimized MUX circuit intellectual property may reduce the critical path delay by about 2.16 ns, and save at lease 3% hardware resources in SDR FPGA.

INDEX TERMS Multiple-Input Multiple-Output, Antenna Selection, Software Defined Radio, FPGA

I. INTRODUCTION

In recent years, multiple-input-multiple-output (MIMO) technology has been paid substantial attention for the fifth generation (5G) wireless communication systems due to its capability of increasing bandwidth efficiency and reliability [1]. However, conventional MIMO systems employ the same number of antennas and radio frequency (RF) chains, implying that enlarging the scale of MIMO system needs to increase both the number of antennas and RF chains simultaneously, which may lead to significantly high power consumption and exorbitant hardware costs. As a remedy, antenna selection (AS) is tailored to alleviate the critical requirements of RF chains in MIMO systems, especially in massive MIMO systems, while retaining the MIMO advantages.

Generally, there are two AS criteria, namely the capacity-based AS (CBAS) and norm-based AS (NBAS) [2]. The main idea of CBAS is to select an antenna subset associated with the highest channel capacity. The optimal performance of CBAS may be achieved by ergodic search based methods, which would significantly increase the system computational complexity when the number of antennas increases, and severely limit the applications of CBAS in large-scale MIMO systems [3] [4]. On the other hand, the main idea of NBAS is to selected the antenna subset associated with the highest channel gain, implying that the selected antenna subset may

TABLE 1: The hardware list of Base Station (BS) and Users

Base Station		Users
PXI chassis (PXI-1085)	Controller (PXIe-8135 24GB/s)	PC
	4 MXI-Expresses	1 USRP-RIO (USRP-2943R)
	2 FPGA modules (PXIe-7976)	
8-channel clock distribution accessory (CDA-2990)		
4 USRP-RIOs (USRP-2943R)		

List of Abbreviations

3GPP	3-rd Generation Partnership Project
5G	The 5-th Generation
AGWN	Additive Gaussian White Noise
AS	Antenna Selection
BER	Bit Error Rate
BS	Base Station
CBAS	Capacity-Based Antenna Selection
CE	Channel Estimation
CRC	Cyclic Redundancy Check
CSI	Channel State Information
DL	Downlink
DSP	Digital Signal Processor
EDAS	Euclidean Distance Based Antenna Selection
FIFO	First-In-First-Out
FP	From Panel
FPGA	Field-Programmable Gate Array
JTRAS	Joint Tx and Rx Antenna Selection
LOS	Line Of Sight
LS	Least Square
LTE	Long Term Evolution
LUT	Look-Up-Tables
MAC	Medium Access Control
MIMO	Multiple-Input Multiple-Output
MUX	Multiplexer
NBAS	Norm-Based Antenna Selection
NLOS	Not Line Of Sight
OFDM	Orthogonal Frequency Division Multiplexing
P2P	Peer-to-Peer
PC	Personal computer
PHY	Physical
QAM	Quadrature Amplitude Modulation
QoS	Quality of Service
RAM	Random Access Memories
RF	Radio Frequency
RRH	Remote Radio Head
RxAS	Receive Antenna Selection
SDR	Software Defined Radio
SM	Spatial Modulation
SNR	Signal-to-Noise Ratio
SSK	Space Shift Keying
STBC	Space-Time Block Coding
TDD	Time Division Duplex
TTCE	Two-Tier Channel Estimation
TxAS	Transmit Antenna Selection
UL	Uplink
VHDL	Very-High-Speed Integrated Circuit Hardware Description Language

achieve the maximum signal-to-noise ratio (SNR) [5] [6]. Compared to the CBAS schemes, NBAS is usually preferred since it is capable of achieving comparable performance with CBAS with lower computational complexity. [7] and [8] considered NBAS in transmit (Tx) AS (TxAS) scenario. In particular, max-norm based AS (ASC1), maximum norm difference based AS (ASC2) and hybrid scheme combining ASC1 and ASC2 were proposed for space shift keying (SSK) system in [7], whereas [8] proposed Euclidean distance based AS (EDAS) at transmitter to improve the bit error rate (BER) performance of the MIMO system. In [9] and [10], receive AS (RxAS) schemes were proposed. More explicitly, a novel RxAS-aided spatial modulation MIMO (SM-MIMO) for millimeter-wave communications, was proposed in [9], which was capable of avoiding an overwhelming complexity and achieving considerable performance. [10] proposed a joint RxAS and power allocation scheme for 5G massive MIMO uplink communication, which is capable of promoting energy conservation then improving the good quality of service (QoS). Furthermore, [2], [11] proposed a two-tier channel estimation (TTCE) aided NBAS by jointly selecting Tx and Rx antennas, which showed that by employing joint Tx and Rx AS, the system's performance may be improved, while retaining low hardware costs and computational complexity. Additionally, [12] compared the performance of joint Tx and Rx AS with TxAS and RxAS, which concluded that the diversity order of JTRAS was significantly reduced in the presence of feedback errors. It is worth mentioning that most of the AS researches are only based on theoretical analysis and performance simulations. The corresponding system implementation is hardly seen in such researches due to the hardware limitations. As a remedy, software defined radio (SDR) platform is tailored to break hardware limitation for next generation communication research [13], [14]. In [15]–[18], the concept of software defined radio (SDR) was introduced, which was characterized by reconfigurability, flexibility and modularity. More Specially, in [15], [16], SDR platform was introduced to implement a system module. While [15] utilized ARM-FPGA to implement a partially reconfigurable orthogonal frequency division multiplexing (OFDM) MIMO physical link, where the performance of Alamouti's space-time block coding (STBC) precoding was measured and verified. While [16] implemented spatial modulator in the SDR transmitter platform, which shows that favorable gains with an advantage over traditional techniques. Furthermore, MIMO system was able to implement in the SDR platform [17], [18]. More specifically, [17] proposed SDR-based prototype hardware design for user equipment to verify scheduling produces and sophisticated signal processing algorithms in both physical (PHY) Layer and medium access control (MAC) Layers in 5G. While [18] presented a 5G-oriented ultra-dense distributed MIMO prototype system by using software-defined radios (SDR), which solves problem about timing and frequency synchronization and avoids data loss or error. In these inspirations, it is expecting that with the aid of SDR system, the implementation of MIMO with AS will be efficiently achieved, accelerating the theoretical algorithms

deploying and system prototyping.

Against this background, the novel contribution of this work is that firstly we investigate the low-complexity NBAS algorithm and implement it with the aid of SDR MIMO communication framework. To be more explicit, we build up a MIMO communication SDR platform with the aid of a series of SDR MIMO devices, the graphical programming software – LabVIEW communications, and the National Instruments (NI) LabVIEW communications MIMO application framework. We further implement the low-complexity NBAS aided MIMO communication system in the MIMO SDR communication platform. Secondly, by implementing the NBAS aided SDR MIMO system, we analyze the channel capacity performance of the MIMO system under a realistic communication environment. Finally, a properly designed channel simulation model is integrated into the NBAS aided MIMO system to analyze the impacts of fading channels on the system's performance, and an optimized MUX circuit is implemented to enhance the hardware performance of the field-programmable gate array (FPGA) in term of delay and resource usage.

II. HARDWARE IMPLEMENTATION OF ANTENNA SELECTION

A. THE FRAMEWORK AND MATHEMATICAL MODEL OF MIMO COMMUNICATION BASE ON SDR

In this paper, we utilize the designed MIMO SDR platform for realizing a MIMO-OFDM system with an up to 8-antenna base station (BS) and two single-antenna users, with the aid of LabVIEW communications MIMO application framework (version 1.5) [19]. The corresponding employed hardware devices are listed in TABLE 1.

Fig. 1 depicts the framework of MIMO BS. More specifically, the block of BS HOST runs on the PXIe-8135 Controller of the PXI chassis, which is capable of realizing downlink (DL) data generation, as well as receiving and saving uplink (UL) data from FPGA. The bit processor acts as the central unit for bit processing in transmit and receive processes, packet generation, cyclic redundancy check (CRC) and bits to symbol modulation. The MIMO processor processes the transmitted and received data in frequency-domain. Bit processor and MIMO processor are both based on the PXIe-7976 FPGA modules within PXI chassis as listed in TABLE I. The Remote Radio Head (RRH) Subsystem is consisted of four USRP-RIOs, More specifically, one of the USRP-RIOs is used as splitter, which receives the processed signals from MIMO processor and distributes these signals to all antennas of different USRP-RIOs via peer-to-peer (P2P) transmission in DL signal transmission. Combiner USRP-RIO collects signals from all antennas via P2P transmission and sends these signals towards MIMO processor in UL signal reception. Each of the four USRP-RIOs may realize the OFDM modulation/demodulation and RF signal processing, associated with two antennas and connected to the PXI-chassis by MXI-Expresses. Besides, despite each FPGA module has different clock frequency and latency, the clock distribution accessory (CDA-2990) is capable of synchronizing all the FPGA module in MIMO BS.

The structure of single-antenna user is shown in Fig. 2. As listed in TABLE 1, the single-antenna user is consisted of a USRP-RIO and a personal computer (PC). USER HOST runs as software on PC and it is responsible for data generation and data reception, which is the same as BS HOST. While the USRP-RIO in the user system integrates functions like bits processing, frequency-domain processing, OFDM modulation/demodulation and RF signals processing, owing to low complexity of signal processing at users.

Our 8×2 MIMO-OFDM system based on NI SDR comprises an 8-antenna BS and two single-antenna users mentioned in Fig. 1 and Fig. 2, respectively, where OFDM modulation is introduced to effectively resist interference between waveforms in channel, making signals suitable for high-speed transmission in multi-path and fading channels. In the following, we derive the mathematical modeling of this MIMO system, where the theoretical derivations are the basis for algorithm implementation and performance measurement in subsequent sections. The system adopts time division duplex (TDD) technology to realize full-duplex communication, and utilizes the UL and DL channel reciprocity in TDD technology, avoiding the trouble of CE for both the UL channel and the DL channel and reducing the complexity of user receivers. At the t-th time slot, the reciprocity between UL channel $\mathbf{H}_{\mathrm{UL}}(t) \in \mathbb{C}^{8\times 2}$ and DL channel $\mathbf{H}_{\mathrm{DL}}(t) \in \mathbb{C}^{2\times 8}$ can be formulated by

$$\mathbf{H}_{\mathrm{DL}}(t) = \mathbf{H}_{\mathrm{UL}}^{\mathrm{H}}(t). \tag{1}$$

With the advantages of TDD, UL transmission can carry some pilot signals used for CE, while DL signals are transmitted in a precoded fashion by exploiting the estimated channel. As a result, the receive signal at t-th time slot $\mathbf{y}_u(t) \in \mathbb{C}^{8\times 1}$ in BS in UL transmission can be expressed by the following model

$$\mathbf{y}_u(t) = \mathbf{H}_{\mathrm{UL}}(t)\mathbf{x}_u(t) + \mathbf{v}_u(t), \tag{2}$$

where $\mathbf{x}_u(t) \in \mathbb{C}^{2\times 1}$ denotes the transmitted signals at the t-th time slot and $\mathbf{v}_u(t) \in \mathbb{C}^{8\times 1}$ stands for the additive Gaussian white noise (AGWN), obeying complex Gaussian random distribution with zero-mean and σ_n^2 variance. Moreover, $\mathbf{x}_u(t)$ includes the pilot signal x_p^t, and the receive pilot signal y_p^t can be expressed as

$$y_p^t = H_p^t x_p^t + v_p^t, \tag{3}$$

where H_p^t and v_p^t are the elements of $\mathbf{H}_{\mathrm{UL}}(t)$ and $\mathbf{v}_u(t)$, respectively. According to Eq. (3), least square (LS) estimator can be utilized for channel estimation (CE). And the channel coefficient $\hat{H}_p^t$ is estimated by

$$\hat{H}_p^t = \frac{y_p^t}{x_p^t}. \tag{4}$$

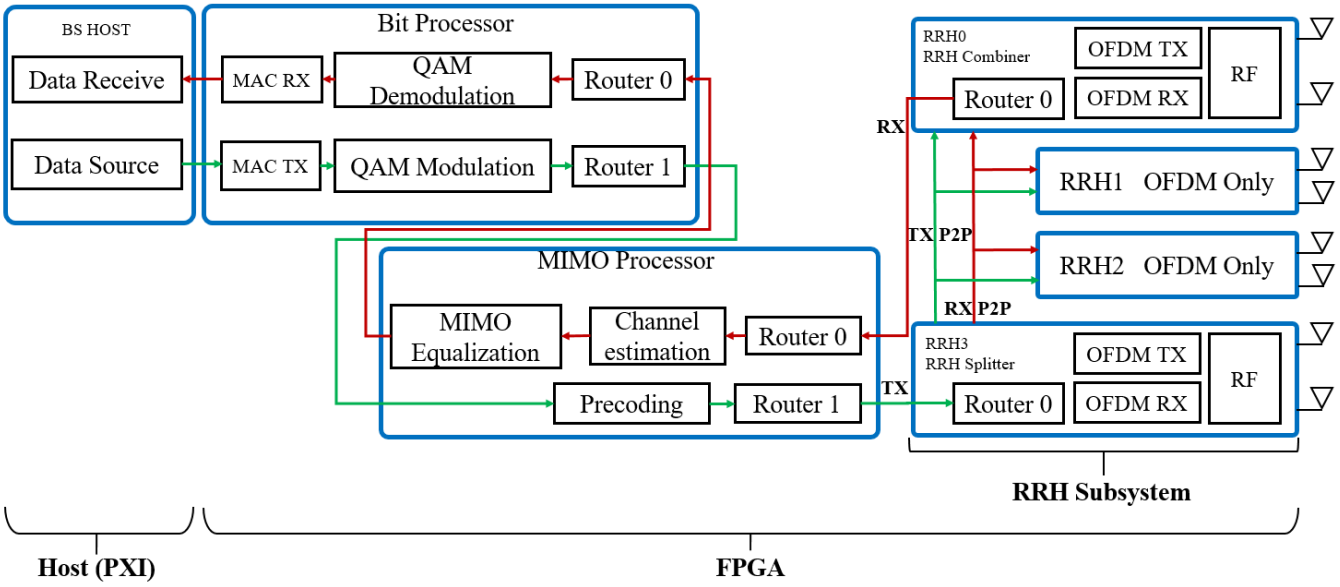

FIGURE 1: The structure of the BS in SDR MIMO communication framework

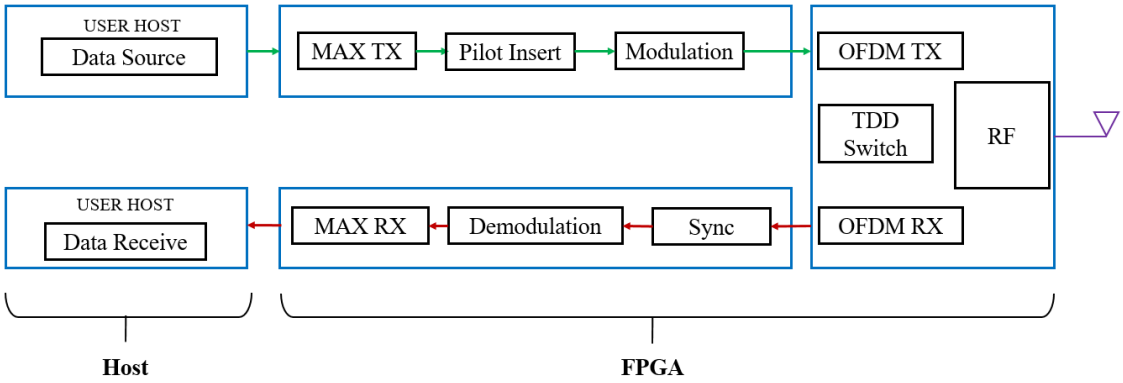

FIGURE 2: The structure of the user in SDR MIMO communication framework.

Then, the whole UL channel can be estimated as $\hat{\mathbf{H}}_{\mathrm{UL}}(t)$. According to Eq. (2), the channel capacity of UL transmission of the NI SDR MIMO system can be expressed as [20], [21]

$$C_{UL}^{t} = \log_2 \det\left(\mathbf{I}_N + \frac{\beta}{M}\hat{\mathbf{H}}_{\mathrm{UL}}(t)\hat{\mathbf{H}}_{\mathrm{UL}}^{\mathrm{H}}(t)\right), \quad (5)$$

where M denotes the number of transmit antennas, β denotes the SNR and $\mathbf{I}_N$ denotes the $N \times N$ identity matrix.

B. THE DESIGN AND IMPLEMENTATION OF ANTENNA SELECTION IN SDR MIMO SYSTEM

In our study, the NBAS algorithm is implemented at BS of NI SDR MIMO-OFDM system. The corresponding block diagram of NBAS-aided MIMO system is shown as Fig. 3, where the RAS information need accurate MIMO channel state information (CSI) determined by CE and the criterion of NBAS can be given as

$$w^* = \arg\max_{w_i \in \mathbf{w}} ||\mathbf{H}_{w_i}||_{\mathrm{F}}^2, \quad (6)$$

where the identifier combination of selected RAs $w^* \in \mathbf{w}^{1\times L}$, where $\mathbf{w}$ denotes indexes of all channel subset $\mathbf{H}_{w_i} \in \mathbb{C}^{N_s \times M}$ and $L = \binom{N}{N_s}$ denotes the number of combinations.

Furthermore, implementation of NBAS requires joint control in both BS HOST and FPGA. BS HOST realizes the theoretical algorithm and the communication performance verification, while FPGA controls the signal processing circuits and antenna RF chains according to NBAS results in BS HOST. As a result, we design three subsystems as shown in Fig. 4 to implement NBAS algorithm in NI SDR MIMO-OFDM system, which are Control Subsystem, NBAS Subsystem and FPGA Control Subsystem. The design details of these three subsystems are introduced as follow.

1) Control Subsystem

Control Subsystem is running on BS HOST, where the main parts are Modules Status Monitor, NBAS Parameters Configuration Controller and Performance Displayer. Firstly, the NBAS Parameters Configuration Controller receives input configuration parameters from users, where these pa-

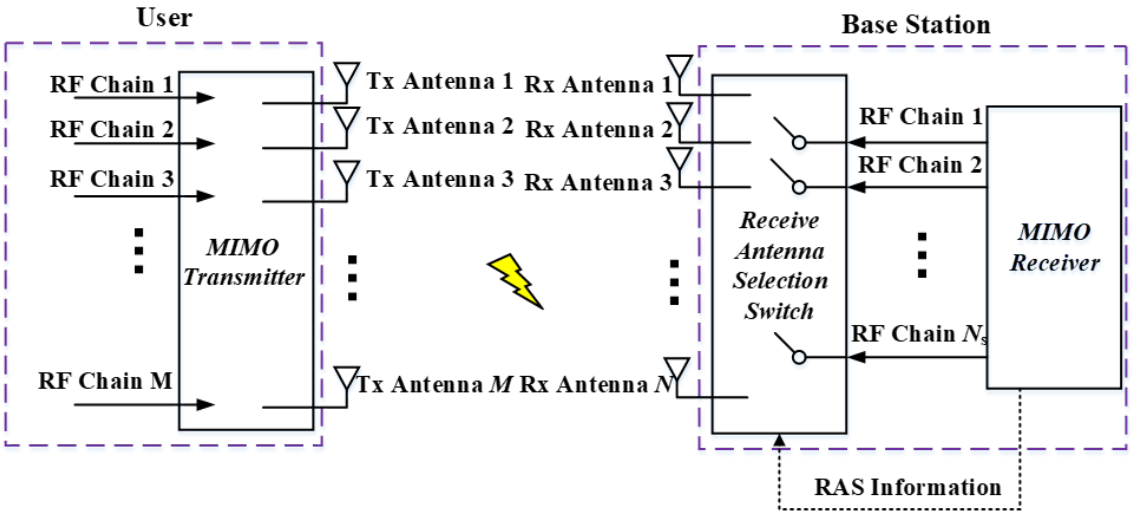

FIGURE 3: The framework of AS-aided MIMO system.

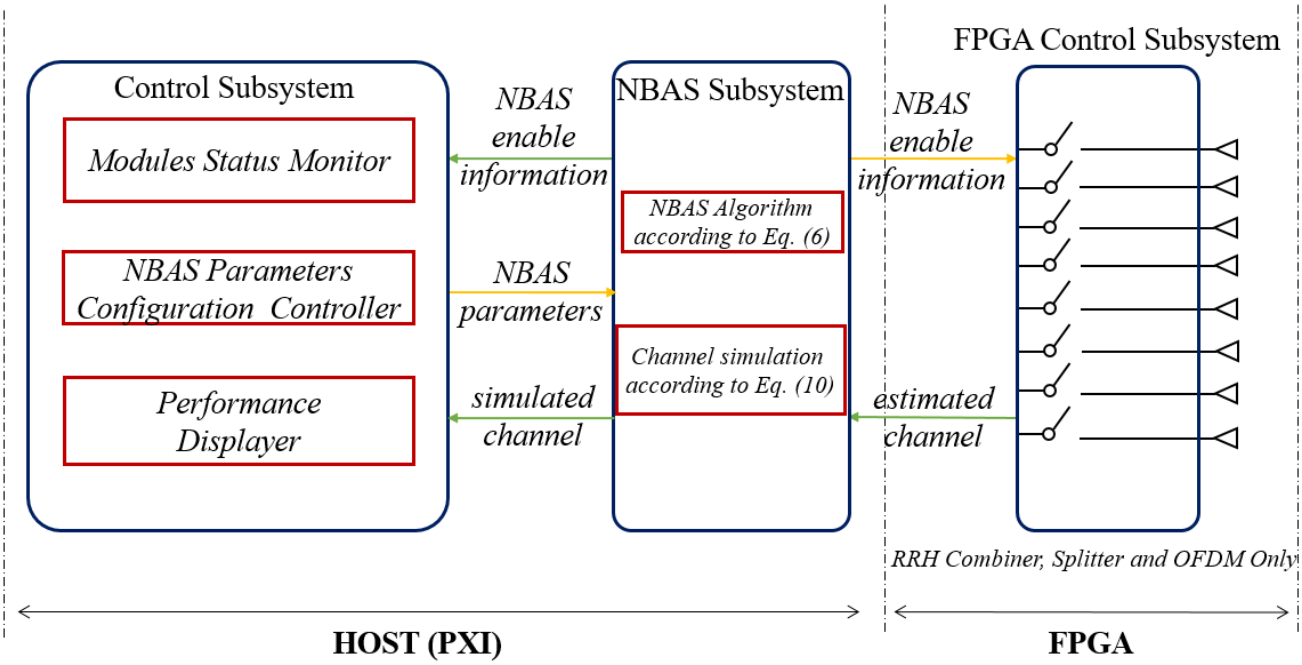

FIGURE 4: The relationship of three subsystems to realize AS in SDR MIMO system

rameters include the number of selected antennas N_s and the status of NBAS activation mode. NBAS activation mode has manual operation and automatic operation modes. The manual mode provides an interface for users, which can determine when to activate NBAS and when to inactivate NBAS, while automatic mode performs automatic NBAS at regular intervals, where users need to input the time interval parameter t_k, where t_k tells the system to re-selects the best antennas according to their real-time energy in every t_k time interval. During system functioning, Modules Status Monitor can display the working status of each module of the system, such as the status of USRP-RIOs and their antennas, which is helpful to check whether the various modules of the system are working properly. In addition, Performance Displayer in the Control Subsystem can demonstrate the real-time performance of the NBAS-aided NI SDR MIMO-OFDM system so that it is great to verify the correctness of the NBAS algorithm as well as measure the gain under the NBAS algorithm on the MIMO-OFDM system.

2) NBAS Subsystem

NBAS Subsystem realizes the NBAS algorithm on BS HOST. In this paper, NBAS is implemented in the NI SDR MIMO framework owing to its low computational complexity. Fig. 5 shows the steps of how NBAS works in the MIMO-OFDM system.

The pilot signals are firstly generated in BS for CE in a 10-millisecond radio frame. Refer to the long-term evolution

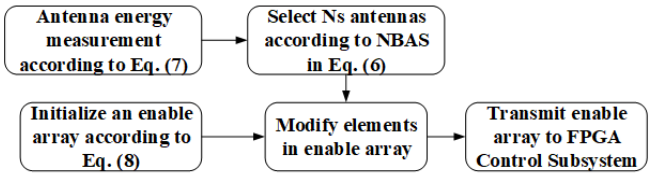

FIGURE 5: The process of NBAS.

(LTE) standard TS36.211 [22] of the 3-rd generation partnership project (3GPP), there are 1200 OFDM subcarriers in a 10-millisecond radio frame. As a result, the energy of i-th antenna can be given as

$$P_i = \sum_{s=1}^{1200} \hat{\mathbf{H}}(i, s), \tag{7}$$

where $i = 0, 1, \cdots, 7$ and $\hat{\mathbf{H}} \in \mathbb{C}^{8\times 1200}$ represents the estimated channel in a 10-millisecond radio frame. If the number of selected antennas is set to N_s, N_s antennas in better energy condition would be selected. Meanwhile, an enable array $\mathbf{e}$ was initialized by

$$\mathbf{e} = \underbrace{[F, F, \cdots, F]}_{N=8}, \tag{8}$$

where F and T denote the boolean values $false$ and $true$, respectively. The boolean array is utilized to set the control signals of whether the antennas in BS is activated or deactivated, where the indexes corresponds to the identifiers of antennas at BS. The relationship between the HOST index of enable array, addresses of USRP-RIOs and antenna identifier is shown in TABLE 2. After NBAS, the elements of the enable array corresponding to the selected antennas are set to T. For example, the total number of antennas N in our MIMO-OFDM system is 8, if N_s = 2 and the No. 0 antenna and the No. 7 antenna are selected, the $\mathbf{e}$ is updated as

$$\mathbf{e} = [T, F, F, F, F, F, F, T]. \tag{9}$$

Then, the updated enable array $\mathbf{e}$ is transmitted to FPGA Control Subsystem through from panel (FP) transmission, which is the module used to control FPGA variables in HOST module in LabVIEW. The transmit process of the enable array is shown in Alg. 1. According to TABLE 2, NBAS enable information are transmitted to the corresponding USRP-RIOs in FPGA Control Subsystem through the FP transmission so that the data links of antennas are in control by NBAS Subsystem. For example, the 0-th and the 1-st enable information in enable array should be transmitted to FPGA to control the corresponding 0-th antenna and 1-st antenna. And USRP-RIO addressed as "USRP01" manages these two antennas. As a result, the 0-th and the 1-st enable information should be sent to "USRP01" for controlling the 0-th antenna and the 1-st antenna, respectively.

3) FPGA Control Subsystem

FPGA Control Subsystem is running on the FPGA of each USRP-RIO. It has been mentioned that the NBAS Subsystem transmits the NBAS enable signals to the FPGA Control Subsystem via FP transmission. Then, each FPGA Control Subsystem can control the data links of their USRP-RIO based on the received signals of $\mathbf{e}$. The method for data link control is to regulate the data output in first-input-first-output (FIFO). More specifically, in each USRP-RIO, the data links of selected antennas, which the control signal of $\boldsymbol{e}$ is T, stay connecting, while those of unselected antennas, which the control signal is F, are cut off. Data in disconnected antenna data links need to keep forward to prevent blocking the FIFO.

Algorithm 1 Process of the enable array transmission towards FPGA Control Subsystem

1: **if** NBAS algorithm is active **then**
2: Updated the enable array $\mathbf{e}$ in Eq. (8) according to NBAS result according to Eq. (6).
3: **else**
4: Set all elements of enable array $\mathbf{e}$ in Eq. (8) to T
5: **end if**
6: Get the addresses of USRP-RIOs
7: Set the corresponding elements of enable array to RIO address to according to TABLE 2
8: Transmit updated enable array $\mathbf{e}$ to FPGA Control Subsystem in USRP-RIOs via FP

TABLE 2: Corresponding relationship of enable array, antenna identifier and USRP-RIO address

HOST	FPGA	
Index of enable array	USRP-RIO address	Antenna identifier
0	USRP 01	0
1		1
2	USRP 02	2
3		3
4	USRP 03	4
5		5
6	USRP 04	6
7		7

C. IMPROVEMENT ON NBAS-AIDED MIMO-OFDM SYSTEM

By exploiting the three subsystems mentioned above, a NBAS-aided NI SDR MIMO-OFDM system is constructed. In this section, we proposed two ways to further improve the performance of the system. Firstly, owing to fixed location of the hardware device, the transmission channel is very stable. Therefore, a channel simulation model is embedded into the NBAS-aided NI SDR MIMO-OFDM system to analyze the impact of fading channels. It is necessary to simulate NBAS under time-varying fading channels and enrich our simulated conditions to further explain the performance enhancement of NBAS in MIMO-OFDM system. Secondly, the initial method of data links control in FPGA Control Subsystem is available but unsafe, since it draws forth data in disconnected data links, which results in data overflow and data loss. Therefore, an optimised MUX module is proposed to control the data link in FPGA Control System. The optimised MUX

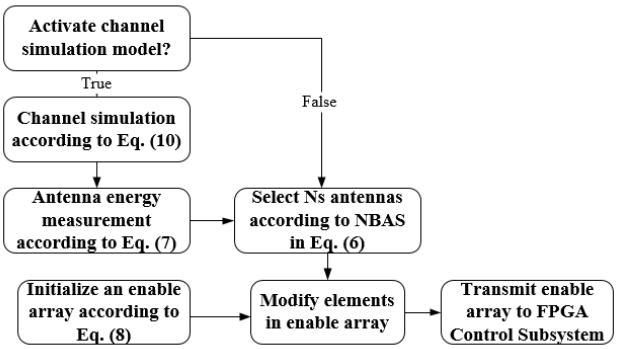

FIGURE 6: The process of NBAS after using channel simulation model

meets the complicated circuit timing in FPGA and it achieves the same function of data link control. Moreover, it is much safer than our initial method by using default selector module in LabVIEW. Focusing on these two aspects of improvements, channel simulation model and self-designed MUX circuit are introduced in our constructed system.

1) Channel Simulation Model

The channel simulation model is embedded into the NBAS Subsystem as shown in Fig. 4. The mathematical model of channels in wireless communication is usually divided into Rayleigh channel model and Rice channel model [23]. In our study, we want to describe environment of multi-path effect and selective fading to simulate the realistic and general wireless communication environments, and Rayleigh channel model is considered [24]. As a result, a baseband channel simulation model is considered. And the simulated channel $\hat{\mathbf{H}}_{sim}$ can be expressed by

$$\hat{\mathbf{H}}_{sim} = \rho\hat{\mathbf{H}}, \tag{10}$$

where $\hat{\mathbf{H}}$ denotes the estimated channel according to Eq. (4) and $\rho \in \mathbb{C}$ stands for the Rayleigh coefficient obeying the Rayleigh distribution with zero-mean and unitary-variance. A designed trigger in the NBAS Subsystem can generate the ρ every t_s seconds, where t_s can be determined by users. Through a Rayleigh coefficient generator, the system is able to communicate under simulated time-varying channels. By changing the value of t_s, the NBAS-aided MIMO-OFDM system can run between fast-varying and slow-varying channels. Fig. 6 has shown the process of NBAS after integrating channel simulation model.

2) Self-Designed Circuit IP

The structure of the default MUX in LabVIEW is shown in Fig. 7-(a), where the selector inputs a boolean value, which is one of the control signals transmitted from NBAS Subsystem. The true case outputs when the value of selector is T, while false case outputs with F in selector. In order to implement the data link control in FPGA Control Subsystem, the information data is connected to the true case input while

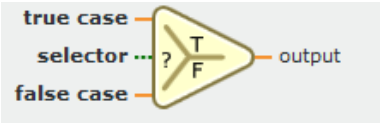

(a) Default MUX in LabVIEW

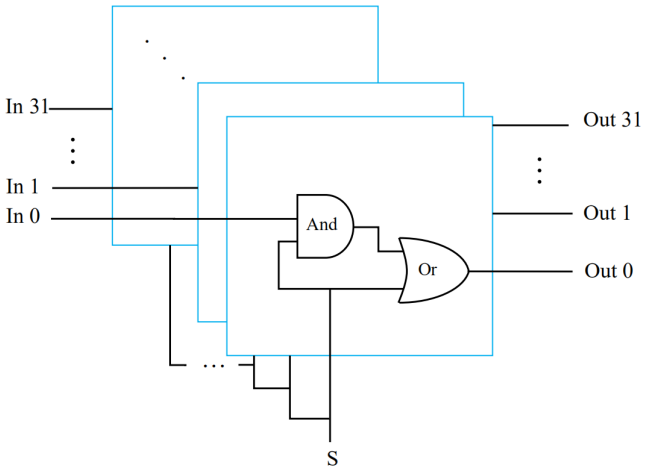

(b) The circuit of self-designed MUX.

FIGURE 7: The structure of different MUXs in FPGA.

zero constant is connected to the false case input. Then, The LabVIEW FPGA compiler is successful in both RRH Splitter and RRH OFDM Only. However, in RRH Combiner module, the 32-bit data transmit through the default MUX of LabVIEW causes extra delay in circuit, which exceeds the data path delay, resulting the RRH Combiner of the MIMO-OFDM system does not meet the timing requirements of FPGA.

To solve this problem, a self-designed 32-bit MUX is designed by using VHDL, where inputs and outputs are assigned in a parallel way as shown in Fig. 7-(b), resulting in reducing data path in FPGA and increasing computation time. The self-designed MUX is loaded into our constructed NBAS-aided MIMO system through "external FPGA IP interface" tool in LabVIEW to replace the default MUX for data link control. Besides, the working logic of optimised MUX is detailed in Alg. 2.

Algorithm 2 Working logic of optimised MUX

```
Get control signals e_i
if e_i = T then
    Assign 32-bit result from input to output
else
    Assign zero to 32-bit output
end if
```

III. EXPERIMENT RESULTS AND ANALYSIS

Our experiments are based on the constructed NBAS-aided NI SDR MIMO-OFDM communication system as introduced in Section II, where the correctness of NBAS algorithm and the performance of NBAS in MIMO system

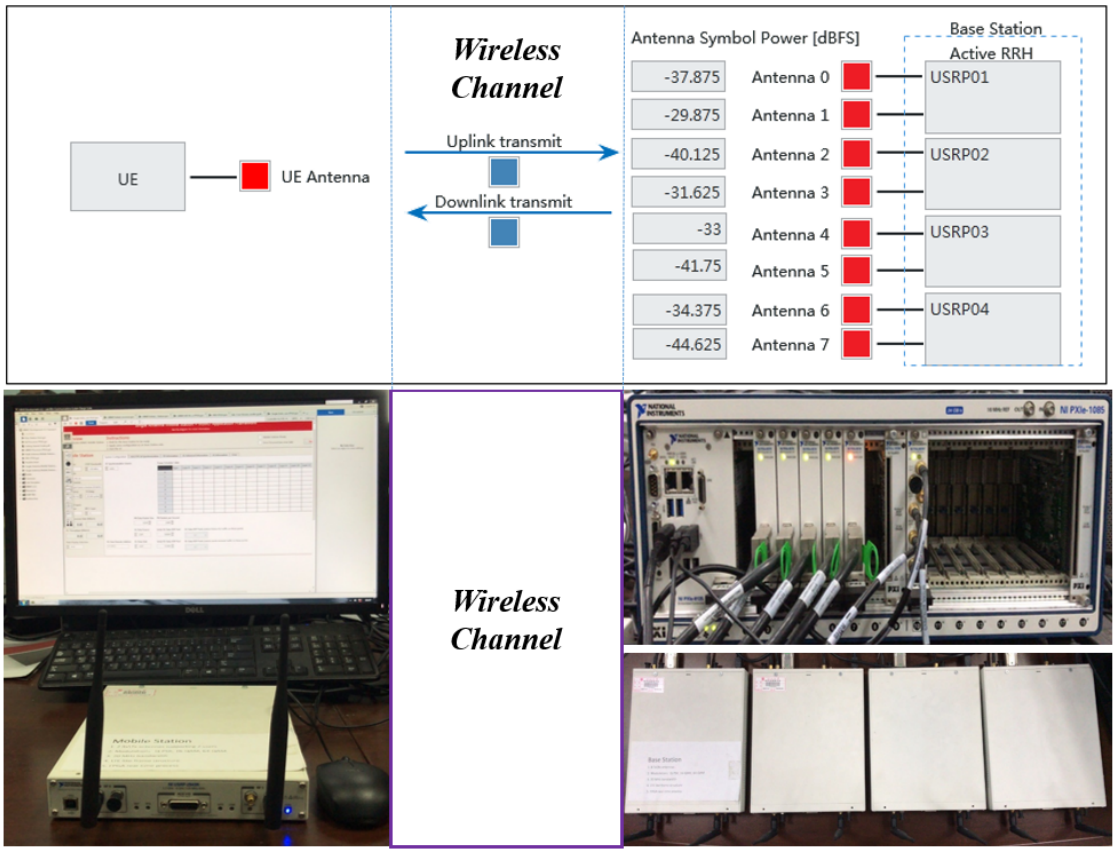

FIGURE 8: Module Status Monitor and the corresponding hardware: single-antenna user and 8-antenna BS

are verified and measured, respectively in this Section under different environments. Section III-A compares the results running on NBAS-aided NI SDR MIMO system against the simulation results from MATLAB while Section III-B shows results running on NBAS-aided NI SDR MIMO-OFDM system with the effect of channel simulation model. Moreover, FPGA hardware performance analysis is performed in Section III-C when considering the self-designed MUX module.

A. VERIFICATION OF NBAS IN MIMO COMMUNICATION

Our constructed NBAS-aided MIMO-OFDM system employs an 8-antenna BS and two single-antenna users (use one USRP-RIO to run as two users). During system functioning, Module Status Monitor in Control Subsystem from Fig. 4 and the corresponding hardware devices listed in TABLE 1 are shown Fig. 8. Besides, system parameters are shown in TABLE 3. Details about these parameters can be found from reference [19].

In order to prove that NBAS algorithm enhances performance of MIMO-OFDM system, different antenna settings for MIMO-OFDM systems with and without NBAS are constructed to calculate channel capacities and the capacity curves are shown in the Performance Displayer of Control Subsystem. In our experiments, $N = N_s = 2$ and $N = N_s = 4$ MIMO-OFDM systems without NBAS are considered, while the corresponding $N = 8$, $N_s = 2$ and $N = 8$, $N_s = 4$ NBAS-aided MIMO-OFDM system with NBAS are constructed to show the performance improvement. The calculations for channel capacity is based on Eq. (5). To further prove the performance of the NBAS-aided NI SDR MIMO-OFDM system, Monte-Carlo simulated capacity curves, which are averaged over 1000 channel realisations, are plotted by MATLAB as comparison. Moreover, the percentage of channel capacity gain η is introduced to quantify the capacity gain in NBAS-aided NI SDR MIMO-OFDM system, which can be expressed by

$$\eta = \frac{C_i - C_g}{C_g} = \frac{G}{G_g}, \tag{11}$$

where C_i denotes the instantaneous channel capacity of the NBAS-aided NI SDR MIMO-OFDM system, whereas C_g denotes that of MIMO-OFDM system without NBAS, where $N = N_s$. And $G = C_i - C_g$ denotes the channel capacity gain.

Antenna energy is measured in FPGA according to Eq. (7) and transmit to Performance Displayer in Control Subsystem, displaying as histogram figure. The energy of i-th antenna P_i is expressed by $10\log_2(P_i/P_{max})$, where P_{max} represents the maximum energy that NBAS-aided NI SDR MIMO-OFDM system can achieve. By comparing the antenna energy of the MIMO system with or without NBAS, the correctness of NBAS can be verified. Fig. 9-(a) displays the antenna energy of $N = N_s = 8$ MIMO-OFDM system

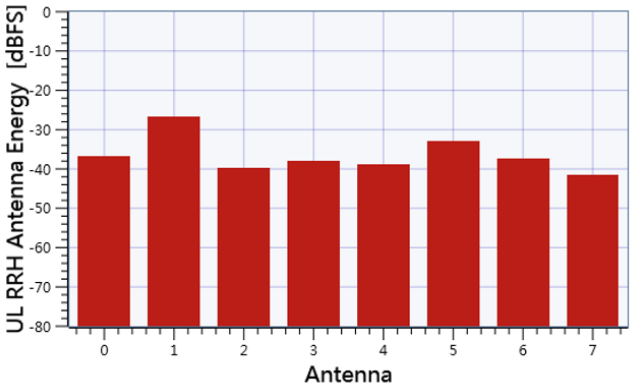

(a) Before NBAS

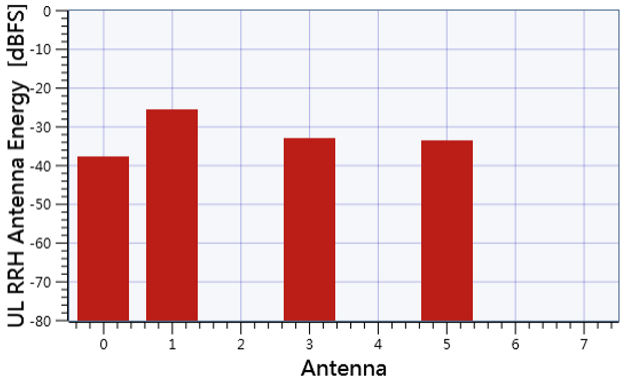

(b) After NBAS

FIGURE 9: The antenna energy comparison of NBAS-aided $N = 8$, $N_s = 4$ MIMO system before NBAS with that after NBAS.

TABLE 3: Signal Parameter

Parameter	Value
Numbers of Users	2
Numbers of users antennas	1
Numbers of BS antennas	8
Bandwidth	120MHz
Carrier frequency	3.610GHz
Sample frequency	30.72MHz
FFT size	2048
Modulation	QPSK
Precoding	Zero Force

without NBAS and Fig. 9-(b) is the result for $N = 8$, $N_s = 4$ NBAS-aided MIMO-OFDM system. It is obvious that No. 0, No. 1, No. 3 and No. 5 antennas are the 4 antennas with the highest antenna energy in 9-(a), while these 4 antennas are perfectly selected in 9-(b), which well proves the correctness of our designed NBAS in MIMO-OFDM system.

Fig. 10 depicts the corresponding channel capacities when considering the 8 antenna energy state in Fig. 9-(a) and 4 selected antenna energy state of in Fig. 9-(b), respectively. From Fig. 10-(a), the instantaneous channel capacity curve and average channel capacity curve of $N = N_s = 8$ MIMO-OFDM system are very close, implying that our simulation of average channel capacity matches the actual

(a) Instantaneous and average capacity comparison of full MIMO-OFDM system.

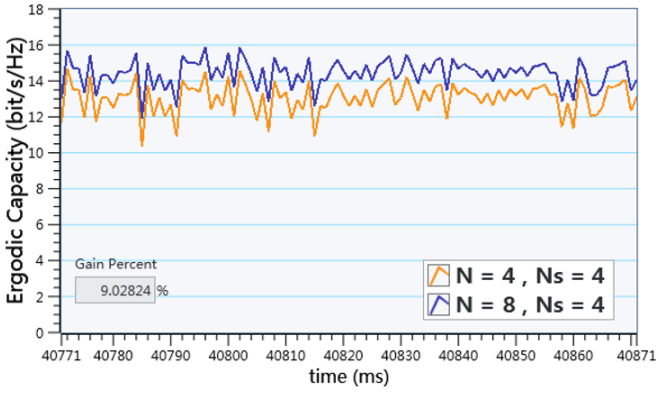

(b) Capacity comparison between NBAS-aided and full MIMO-OFDM system.

FIGURE 10: Corresponding channel capacity of Fig. 9.

transmission environment. For example, in Fig. 10-(a), the channel capacity is around 16 bits/s/Hz at the 39220-th ms, while the average value is about 16.2 bits/s/Hz, which shows 0.2 bits/s/Hz capacity loss, implying that the current channel link state is slightly worse than the average. Fig. 10-(b) illustrates $N = 8$, $N_s = 4$ NBAS-aided MIMO-OFDM system have capacity gain when compared with $N = N_s = 4$ MIMO-OFDM system. More specifically, the capacity of $N = 8$, $N_s = 4$ NBAS-aided MIMO-OFDM system is approximately 14 bits/s/Hz at the 40871-th ms, compared with 12.8 bits/s/Hz value of $N = N_s = 4$ MIMO-OFDM system, which shows around 9% capacity gain according to Eq. (11).

In our experiments, SNR can be adjusted by changing the direction of antennas, adding obstacles in the wireless communication environment in order to add noise to plot the measured channel capacity vs. SNR curves. Fig. 11 shows the comparison of channel capacity vs. SNR curves between $N = 8$, $N_s = 4$ NBAS-aided MIMO-OFDM system and $N = N_s = 4$ MIMO-OFDM system both in simulation and measurement, respectively. Channel capacity from MATLAB simulations are shown in Fig. 11-(a) and measurements from NBAS-aied MIMO-OFDM system are plotted in Fig. 11-(b). The channel capacity results of $N = 8$, $N_s = 4$ NBAS-

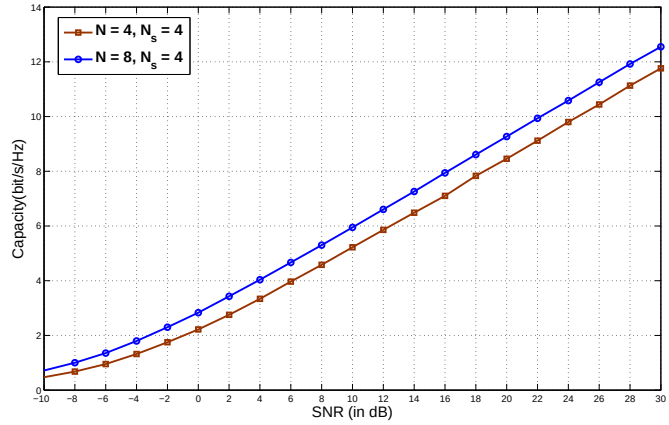

(a) Capacity Simulation in MATLAB

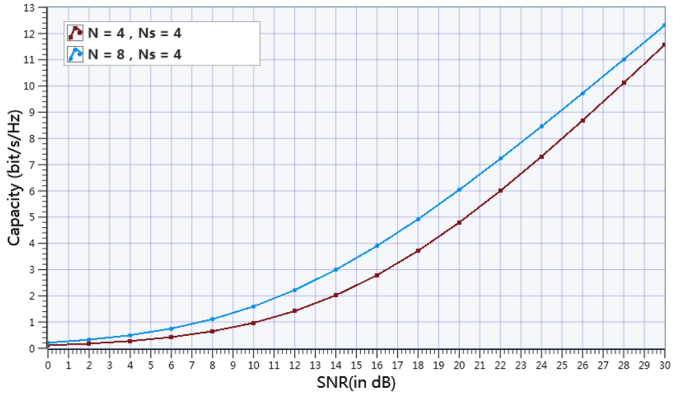

(b) Capacity Measurement in NBAS-aided MIMO system

FIGURE 11: Channel capacity comparison of NBAS aided-$N = 8$, $N_s = 4$ MIMO-OFDM system and $N = N_s = 4$ MIMO-OFDM system under simulation and realistic measurement.

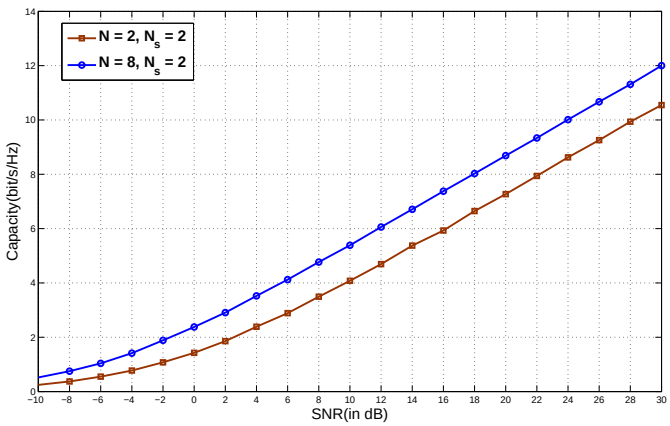

(a) Capacity Simulation in MATLAB

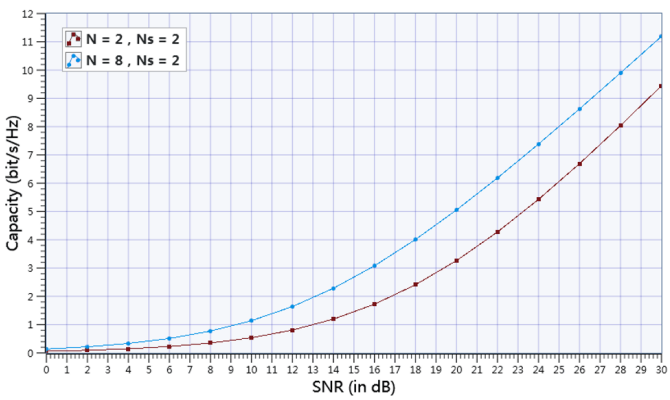

(b) Capacity Measurement in NBAS-aided MIMO-OFDM system

FIGURE 12: Channel capacity comparison of NBAS aided-$N = 8$, $N_s = 2$ MIMO-OFDM system and $N = N_s = 2$ MIMO-OFDM system under simulation and realistic measurement.

aided MIMO-OFDM system shows better capacity across SNR from 0 dB to 30 dB than that of the $N = N_s = 4$ MIMO-OFDM system in both Fig. 11-(a) and Fig. 11-(b). More specifically, the simulated capacity of $N = 8$, $N_s = 4$ NBAS-aided MIMO-OFDM system reaches 12.55 bits/s/Hz and that of $N = N_s = 4$ MIMO-OFDM system is 11.76 bits/s/Hz when SNR = 30 dB in Fig. 11-(a), which shows 9% channel capacity gain according to Eq. (11). While in Fig. 11-(b) the measured capacity of $N = 8$, $N_s = 4$ NBAS-aided MIMO-OFDM system is 12.4 bits/s/Hz and that of $N = N_s = 4$ MIMO-OFDM system is 11.5 bits/s/Hz, which has the same 9% channel capacity gain when compared to the simulation results shown in Fig. 11-(a).

To further prove the same trend of channel capacity gain between simulation and measurement, Fig. 12 depicts the channel capacity vs. SNR curves comparison between $N = 8$, $N_s = 2$ NBAS-aided MIMO-OFDM system and $N = N_s = 2$ MIMO-OFDM system, where capacity simulations are shown as Fig. 12-(a) and measurements are shown as Fig. 12-(b). Similarly, the measured channel capacity gain is 15% when SNR = 30 dB as shown in Fig. 12-(b), which also agrees with the 14% of simulated channel capacity gain in Fig. 12-(a). It is interesting to observe that the 15% capacity gain of $N = 8$, $N_s = 2$ NBAS-aided MIMO-OFDM system is higher than 9% of $N = 8$, $N_s = 4$ NBAS-aided MIMO-OFDM system, this is because the $N = 8$, $N_s = 2$ NBAS-aided MIMO-OFDM systems has the largest AS factor $f_{AS} = 4$ according to Eq. (12), implying the best effect of selection is accessible.

$$f_{AS} = \frac{N}{N_s}. \tag{12}$$

B. ANALYSIS OF CHANNEL SIMULATIONS

According to Eq. (10), the channel simulation model generates a ρ every t_s seconds, which can simulated time-varying channels. In time-varying channels, CSI changes over time. In order to maintain a high system performance gain, periodic CE and NBAS are required. In our experiments, time-varying interval t_s is introduced to control the changing speed of the channel. While automatic NBAS mode is used to increase frequency of CE and NBAS, where NBAS interval parameter t_k is introduced to control the frequency of CE and NBAS.

TABLE 4: The comparison of FPGA total slices occupation between self-designed MUX and default MUX

Type of USRP-RIO	Self-designed MUX		Default MUX		Total Slice
	Used	Percentage	Used	Percentage	
RRH OFDM Only	23,566	37%	24,149	38%	63,550
RRH Splitter	30,885	49%	30,885	49%	63,550
RRH Combiner	30,652	48%	32,411	51%	63,550

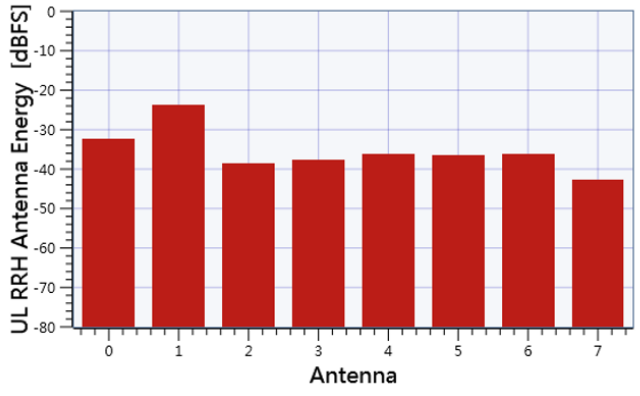

(a) Realistic environment

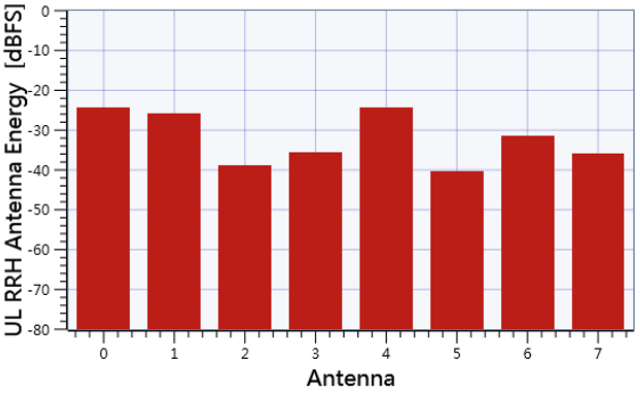

(b) Simulated fading environment

FIGURE 13: Antenna energy comparison in realistic and simulated fading communication environments.

Moreover, t_s and t_k can be set to any values according to different scenario. For convenient measurements and smooth system operation, t_s and t_k are both set to 20 ms to achieve system balance.

Fig. 13 portrays the the status of 8 antennas in the system from the realistic energy of antennas to the fading energy of antennas, where Fig. 13-(a) shows the realistic energy of antennas, and Fig. 13-(b) displays the fading energy of antennas due to the effect of channel simulation model. From Fig. 13, the antenna energy in realistic case differs from that in fading case, owing to Rayleigh fading coefficients is considered, which can utilize the fading antenna energy to simulate the Rayleigh fading environment.

According to Eq. (11), Fig. 14 depicts the channel capacity gain G of $N = 8$, $N_s = 4$ NBAS-aided MIMO system with the setting of $t_s = t_k = 20$ ms and enabled automatic

TABLE 5: Timing comparison between self-designed MUX and default MUX in RRH Combiner

Type / Timing	Self-designed MUX	Default MUX
Max Critical Path(ns)	4.49	6.65
Max Frequency(MHz)	200	150

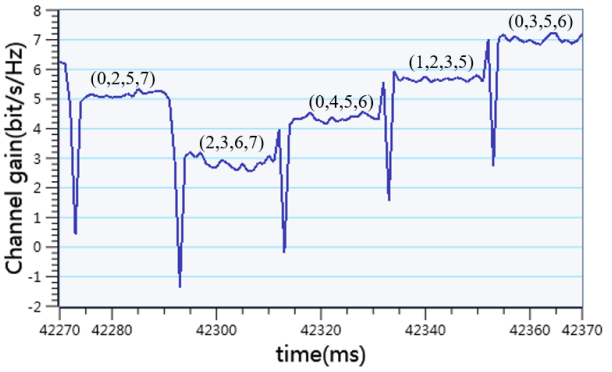

FIGURE 14: The channel capacity gain of auto AS mode in simulated fading environment.

NBAS mode. From Fig. 14 we can observe that there will be a downward pulse every 20 ms, which means all antenna links need to be turned on for CE and update the CSI at this moment. Furthermore, the NBAS in every 20 ms period is capable of maintaining higher channel capacity gain in the $N = 8$, $N_s = 4$ NBAS-aided MIMO system. More specifically, in the period of 42274-th ms to 42294-th ms, the number of selected antennas is $(0, 2, 5, 7)$ and the channel capacity gain has maintained 5.1 bits/s/Hz, while in the next period, saying the period of 42294-th ms to 42314-th ms, the number of selected antennas is $(2, 3, 6, 7)$, which maintained around 3 bits/s/Hz channel capacity gain. The variety of channel capacity gain is because different Rayleigh fading coefficients in Eq. (10) are generated every 20 ms.

C. PERFORMANCE ANALYSIS OF FPGA

By using the self-designed MUX circuit module introduced in Section II-C, usage of hardware resource of FPGA in USRP-RIO can be reduced. TABLE 4 is the comparison of FPGA total slices usage between default MUX and self-designed MUX. It shows results for three different RRH modules from Fig. 1 that run in FPGA of USRP-RIOs: OFDM Only, RRH Splitter and RRH Combiner. In TABLE 4, the FPGA total slices usage of OFDM only module is reduced by 1%, while the FPGA total slices usage of Combiner module

TABLE 6: FPGA Utilization

Property \ Type		USRP-RIO 1 RRH Splitter	USRP-RIO 2 - 3 RRH OFDM-Only	USRP-RIO 4 RRH Combiner	PXIe FPGA 1 MIMO Processor	PXIe FPGA 2 Bit Processor
Registers	Used	102,888	92,282	116,637	209,368	112,737
	Percentage	21%	18%	23%	41%	22%
DSPs	Used	388	388	452	1,084	12
	Percentage	25%	25%	29%	70%	1%
Block RAMs	Used	317	236	313	630	343
	Percentage	40%	30%	39%	84%	43%
LUTs	Used	63,427	54,144	74,112	155,277	104,026
	Percentage	25%	21%	29%	61%	41%
Total Slices	Used	30,885	23,566	30,652	58,238	39,283
	Percentage	49%	37%	48%	92%	62%
Maximum Frequency		200MHz	200MHz	200MHz	200MHz	200MHz

is further reduced by 3%. Moreover, in TABLE 5, results indicate the self-designed MUX circuit in RRH Combiner module can reduce the critical path delay from 6.65 ns while using default MUX to 4.49 ns by using self-designed MUX, which provides faster running time and meets the requirement of system operating frequency 200 MHz for the FPGA hardware. Finally, after applying the self-designed MUX circuit, the total FPGA resource utilization about registers, digital signal processors (DSPs), block random-access memories (RAMs) and look-up-tables (LUTs), total slices as well as FPGA maximum frequency is listed in TABLE 6. More specifically, RRH Splitter, RRH Combiner, RRH OFDM-Only, as mentioned in Section II-A, are run in different USRP-RIOs. While MIMO Processor and Bit Processor are run on different FPGA modules (PXIe-7976) in PXI chassis. The USRP-RIOs and PXIe-7976 both use the same Xilinx Kintex-7-410T FPGA, therefore they provide the same amout of FPGA resource for different modules. For example, results in TABLE 6 show that 102,888 registers are used in RRH Splitter of our constructed system, which accounts for 21% of the registers available in USRP-RIO 1. While 209,368 registers are used in MIMO Processor and accounting for 41% of the total number of the registers in PXIe FPGA 1.

IV. CONCLUSIONS

In this paper, a NBAS-aided MIMO-OFDM system base on NI SDR is designed and implemented. In the experimental results, the channel capacity is measured to verify the performance gain in NBAS-aided MIMO-OFDM system. The capacity of NBAS-aided MIMO-OFDM system is higher than that of MIMO-OFDM system without NBAS, as shown in Fig. 12, the $N = 8$, $N_s = 2$ NBAS-aided MIMO-OFDM system has the largest performance improvement, which increases 15% capacity gain when compared to $N = N_s = 2$ MIMO system without NBAS. In addition, a channel simulation model is embedded into the implemented system to check the NBAS-aided MIMO-OFDM communication performance under the impact of fading channel. Results in Fig. 14 show that with the effect of time-varying channel, the NBAS algorithm always selects the antennas with highest energy to keep the system in better performance. Last but not least, a self-designed MUX circuit module is import into the FPGA in NBAS-aided MIMO-OFDM system to reduce the hardware usage and improve the operating speed of hardware circuit. There are large amount of researches study the AS algorithm but to the best of our knowledge, our implemented NBAS-aided NI SDR MIMO-OFDM system is the first hardware system that provides a near-realistic MIMO communication system to run with NBAS algorithm. With the help of our system, the design and evolution of new AS algorithm in MIMO system can be verified in a practical environment, which will help the development of next generation communication systems. To achieve this target, we have uploaded our source code to Github [25].

REFERENCES

[1] L. Dong et al., "Introduction on IMT-2020 5G Trials in China," in IEEE Journal on Selected Areas in Communications, vol. 35, no. 8, pp. 1849-1866, Aug. 2017.

[2] P. Zhang, S. Chen and L. Hanzo, "Two-Tier Channel Estimation Aided Near-Capacity MIMO Transceivers Relying on Norm-Based Joint Transmit and Receive Antenna Selection," in IEEE Transactions on Wireless Communications, vol. 14, no. 1, pp. 122-137, Jan. 2015.

[3] X. Wang, L. Xiao, Y. Zhang and Z. He, "Measurement-Based Massive MIMO Antenna Selection in Indoor Office Scenario at 3.52 GHz," 2018 IEEE 18th International Conference on Communication Technology (ICCT), Chongqing, 2018, pp. 573-577.

[4] Y. Gao, H. Vinck and T. Kaiser, "Massive MIMO Antenna Selection: Switching Architectures, Capacity Bounds, and Optimal Antenna Selection Algorithms," in IEEE Transactions on Signal Processing, vol. 66, no. 5, pp. 1346-1360, March, 2018.

[5] A. Yilmaz and O. Kucur, "Error performance of joint transmit and receive antenna selection in two hop amplify-and-forward relay system over Nakagami-mfading channels," in Proc. IEEE 21st PIMRC, Istanbul, Turkey, Sep. 26-29, 2010, pp. 2198-2203.

[6] T. Gucluoglu and T. M. Duman, "Space-time coded systems with joint transmit and receive antenna selection," in Proc. IEEE ICC, Glasgow, U.K., Jun. 24-28, 2007, pp. 5305-5310.

[7] W. Chung and C. Hung, "Multi-Antenna Selection Using Space Shift Keying in MIMO Systems," 2012 IEEE 75th Vehicular Technology Conference (VTC Spring), Yokohama, 2012, pp. 1-5.

[8] N. Pillay and H. Xu, "Low-complexity transmit antenna selection schemes for spatial modulation," in IET Communications, vol. 9, no. 2, pp. 239-248, 22 1 2015.

[9] P. Yang, Y. Xiao, Y. L. Guan, Z. Liu, S. Li and W. Xiang, "Adaptive SM-MIMO for mmWave Communications With Reduced RF Chains," in IEEE Journal on Selected Areas in Communications, vol. 35, no. 7, pp. 1472-1485, July 2017.

[10] H. Gao, Y. Su, S. Zhang and M. Diao, "Antenna selection and power allocation design for 5G massive MIMO uplink networks," in China Communications, vol. 16, no. 4, pp. 1-15, April 2019.

[11] P. Zhang, S. Chen, C. Dong, L. Li and L. Hanzo, "Norm-based joint transmit/receive antenna selection aided and two-tier channel estimation assisted

STSK systems," 2014 IEEE International Conference on Communications (ICC), Sydney, NSW, 2014, pp. 5049-5054.
[12] A. Yilmaz and O. Kucur, "Performances of Transmit Antenna Selection, Receive Antenna Selection, and Maximal-Ratio-Combining-Based Hybrid Techniques in the Presence of Feedback Errors," in IEEE Transactions on Vehicular Technology, vol. 63, no. 4, pp. 1976-1982, May 2014.
[13] A. De Sabata, C. Balint, P. Bechet and S. Miclaus, "USRP based HF spectrum occupancy measurements at two locations in central and Western Romania," 2017 International Symposium on Signals, Circuits and Systems (ISSCS), Iasi, 2017, pp. 1-4.
[14] G. Soni and G. Megh, "Experimental investigation of spectrum sensing for LTE frequency band based on USRP 2920/VST 5644," 2016 International Conference on Control, Instrumentation, Communication and Computational Technologies (ICCICCT), Kumaracoil, 2016, pp. 801-804.
[15] K. A. Arun Kumar, "ARM-FPGA Implementation of a Partially Reconfigurable OFDM-MIMO Phy-Link," 2018 International CET Conference on Control, Communication, and Computing (IC4), Thiruvananthapuram, 2018, pp. 288-292.
[16] O. Hiari and R. Mesleh, "A Reconfigurable SDR Transmitter Platform Architecture for Space Modulation MIMO Techniques," in IEEE Access, vol. 5, pp. 24214-24228, 2017.
[17] Y. Liu et al., "Multiband User Equipment Prototype Hardware Design for 5G Communications in Sub-6-GHz Band," in IEEE Transactions on Microwave Theory and Techniques, vol. 67, no. 7, pp. 2916-2927, July 2019.
[18] J. Wang, K. Wang, B. Han, S. Zhang, C. Wen and S. Jin, "SDR Implementation of a 5G-Oriented Ultra-Dense Distributed MIMO Prototype System," 2018 10th International Conference on Wireless Communications and Signal Processing (WCSP), Hangzhou, 2018, pp. 1-6.
[19] LabView Communications MIMO Application Framework 1.5 [Online]. Avaliable: http://www.ni.com/download/mimo-application-framework-1.5. Accessed on: Sep. 28, 2018
[20] F. Jin and L. Hanzo, "Ergodic Capacity of Multi-User MIMO Systems Using Pilot-Based Channel Estimation, Quantized Feedback and Outdated Feedback as Well as User Selection," 2012 IEEE Vehicular Technology Conference (VTC Fall), Quebec City, QC, 2012, pp. 1-5.
[21] A. Jain, R. Upadhyay, P. D. Vyavahare and L. D. Arya, "Stochastic Modeling and Performance Evaluation of Fading Channel for Wireless Network Design," 21st International Conference on Advanced Information Networking and Applications Workshops (AINAW'07), Niagara Falls, Ont., 2007, pp. 893-898.
[22] J. Zhang, B. Zhang, S. Chen, X. Mu, M. El-Hajjar and L. Hanzo, "Pilot Contamination Elimination for Large-Scale Multiple-Antenna Aided OFDM Systems," in IEEE Journal of Selected Topics in Signal Processing, vol. 8, no. 5, pp. 759-772, Oct. 2014.
[23] 3GPP LTE TS36.211: Evolved Universal Terrestrial Radio Access (E-UTRA); Physical channels and modulation
[24] V. Tarokh, A. Naguib, N. Seshadri and A. R. Calderbank, "Space-time codes for high data rate wireless communication: performance criteria in the presence of channel estimation errors, mobility, and multiple paths," in IEEE Transactions on Communications, vol. 47, no. 2, pp. 199-207, Feb. 1999.
[25] Source codes for the proposed NBAS aided SDR MIMO system: https://github.com/Junzjam/SDR_LabView.

PEICHANG ZHANG received the B.Eng.degree (Hons.) in electronic engineering from the University of Central Lancashire, Preston,U.K., in 2009, and the M.Sc. and Ph.D. degree in wireless communications from the University of Southampton, Southampton, U.K., in 2010 and 2015, respectively. He is currently with the College of Electronics and Information Engineering, Shenzhen University, China. His research interests include antenna selection, coherent and non-coherent detection, iterative detection, and channel estimation.

JIAJUN XU born in Guangdong, China, 1994. He received the B.Sc. degree in communication engineering from Shenzhen University, Shenzhen, China, in 2017. Since 2017, he has been pursuing a M.Sc. degree in information and communication engineering in Shenzhen University, Shenzhen, China. His current research interests include multiple-input-multiple-output (MIMO) wireless communication, antenna selection, internet of things (IoT), cooperative communication, and joint algorithm and hardware codesign.

SHIDA ZHONG received the B.Sc. degree in electronics engineering from Shenzhen University, Shenzhen, China, in 2008, and the M.Sc. and Ph.D. degrees in electronics and electrical engineering from the University of Southampton, Southampton, U.K., in 2009 and 2013, respectively. From 2013 to 2017, he was a Research Fellow with the School of Electronics and Computer Science, University of Southampton. From 2016 to 2018, he was a Founding Member with the spin-out company AccelerComm Ltd., Southampton. He is currently an Assistant Professor with the College of Electronics and Information Engineering, Shenzhen University. His current research interests include design for testing, antenna selection, joint algorithm and hardware codesign, FPGA and ASIC implementations for next-generation channel coding system.

HAOGANG FENG born in Henan, China, 1997. He received the B.Sc. degree in electronics engineering from Shenzhen University, Shenzhen, China, in 2019. From 2019 on, he will pursue Ph.D. degree in electronics and electrical engineering in Shenzhen University, Shenzhen, China. His current research interests include feld-programmable gate array(FPGA), joint algorithm and hardware codesign, and application-specified integrated circuit(ASIC) implementations for next-generation channel coding system.

LEI HUANG received the B.Sc., M.Sc., and Ph.D. degrees in electronic engineering from Xidian University, Xi'an, China, in 2000, 2003, and 2005, respectively. From 2005 to 2006, he was a Research Associate with the Department of Electrical and Computer Engineering, Duke University, Durham, NC, USA. From 2009 to 2010, he was a Research Fellow with the Department of Electronic Engineering, City University of Hong Kong, Kowloon, Hong Kong, and a Research Associate with the Department of Electronic Engineering, The Chinese University of Hong Kong, Shatin, Hong Kong. From 2011 to 2014, he was a Professor with the Department of Electronic and Information Engineering, Shenzhen Graduate School of Harbin Institute of Technology, Shenzhen, China. In November 2014, he joined the Department of Information Engineering, Shenzhen University, where he is currently a Chair Professor. His research interests include spectral estimation, array signal processing, statistical signal processing, and their applications in radar and wireless communication systems. Dr. Huang is currently serving as an Associate Editor for the IEEE TRANSACTIONS ON SIGNAL PROCESSING and Digital Signal Processing.

TAO YUAN received the Bachelor and Master degrees from Xidian University, China, and the Ph.D. degree from National University of Singapore, Singapore. He is currently a Professor with the College of Electronics and Information Engineering at the Shenzhen University, Shenzhen, China. His current research interests include developing novel RF modules and antennas for mobile terminal and 5G applications.

JIANKANG ZHANG (S'08-M'12-SM'18) received the B.Sc. degree in Mathematics and Applied Mathematics from Beijing University of Posts and Telecommunications in 2006, and the Ph.D. degree in Communication and Information Systems from Zhengzhou University in 2012. Dr Zhang was a lecturer from 2012 to 2013 and an associate professor from 2013 to 2014 in School of Information Engineering, Zhengzhou University. From 2009 to 2011, Dr Zhang was a visiting PhD student in the School of Electronics and Computer Science, the University of Southampton, UK. Currently, he is a Senior Research Fellow in the University of Southampton, UK. Dr Zhang is a recipient of a number of academic awards, including Excellent Doctoral Dissertation of Henan Province, China, Youth Science and Technology Award of Henan Province, China. His research interests are in the areas of wireless communications and signal processing, aeronautical communications and broadband communications. He serves as an Associate Editor for IEEE ACCESS and a guest editor of a special issue on EURASIP Journal on Advances in Signal Processing.